一般化短パルス方程式の多重ソリトン解のパラメータ表示

Parametric representations of multisoliton solutions of the generalized short pulse equations

山口大学大学院創成科学研究科　松野 好雅 (Yoshimasa Matsuno)
Division of Applied Mathematical Science
Graduate School of Sciences and Technology for Innovation
Yamaguchi University, Ube, Yamaguchi 755-8611, Japan
E-mail address: matsuno@yamaguchi-u.ac.jp

Abstract

We consider three novel PDEs associated with the integrable generalizations of the short pulse equation classified recently by Hone *et al* (2018 *Lett. Math. Phys.* **108** 927-947). In particular, we obtain a variety of exact solutions by means of a direct method combined with the reciprocal transformations. We report the main results associated with soliton solutions. Specifically, we present the parametric representations of multisoliton solutions. These solutions include cusp solitons, unbounded solutions with finite slope and breathers. In addition, the cusped periodic wave solutions are constructed from the cusp solitons by means of a simple procedure. The new features of solutions are exemplified for both the cusp solitons and cusped periodic waves.

1. Introduction

The classification of the integrable PDEs of second order with quadratic and cubic nonlinear terms has been performed recently by Hone *et al* [1]. They found the following seven integrable PDEs including the SP equation:

$$u_{xt} = u + \frac{1}{6}(u^3)_{xx}, \tag{1.1}$$

$$u_{xt} = u + (u^2)_{xx}, \tag{1.2}$$

$$u_{xt} = u + 2uu_{xx} + u_x^2, \tag{1.3}$$

$$u_{xt} = u + u^2u_{xx} + uu_x^2, \tag{1.4}$$

$$u_{xt} = u + 4uu_{xx} + u_x^2, \tag{1.5}$$

$$u_{xt} = u + (u^2 - 4u^2u_x)_x, \tag{1.6}$$

$$u_{xt} = u + \alpha(2uu_{xx} + u_x^2) + \beta(u^2u_{xx} + uu_x^2), \quad \alpha\beta \neq 0, \tag{1.7}$$

where $u = u(x,t)$ represents a scalar function of x and t, and subscripts x and t appended to u denote partial differentiations. Equation (1.1) is the short pulse (SP) equation which has been derived as an asymptotic model describing the propagation of ultra-short pulses in isotropic optical fibers [2]. A large number of works have been devoted to the study of the SP equation. See, for example, a review article [3] as for the soliton and periodic solutions and their properties. Equations (1.2), (1.3) and (1.4) are already known and sometimes called the Vakhnenko (or reduced Ostrovsky), Hunter-Suxton and modified SP equations, respectively [4-7]. While equations (1.3) and (1.5) have been derived in the process of studying the short-wave dynamics of surface gravity waves [8], the analysis of the latter equation has not been done yet. On the other hand, equations (1.6) and (1.7) seem to be new, as far as we know.

The purpose of this short report is to present the parametric representations for exact solutions of equations (1.5)-(1.7) and investigate their properties. In particular, we are concerned with the cusp soliton solutions and their periodic analogs for each equation. The detailed description of the exact method of solutions and solutions will be reported elsewhere [9].

2. Parametric solutions of equation (1.5)

First, we rewrite equation (1.5) in the form

$$u_{xt} = \frac{3}{2}\,u - uu_{xx} - \frac{1}{4}\,u_x^2, \tag{2.1}$$

by rescaling the variables according to $t \to (3/2)t, u \to -u/6$. Then, equation (2.1) can be put into the local conservation law

$$p_t + (pu)_x = 0, \quad p = m^{\frac{2}{3}}, \quad m = 1 - u_{xx}. \tag{2.2}$$

We construct solutions of equation (2.1) under the boundary condition $u \to 0,\ |x| \to \infty$.

2.1. Parametric solutions

The goal is to establish the following theorem.

Theorem 2.1. *Equation (2.1) admits the parametric representation for the multisoliton solutions*

$$u = -2(\ln g)_{\tau\tau}, \tag{2.3a}$$

$$x = y - 2(\ln g)_\tau + y_0, \tag{2.3b}$$

where $g = g(y,\tau)$ is the tau-function given by

$$g = f^2 - 2D_\tau D_y f \cdot f, \tag{2.4}$$

with $f = f(y,\tau)$ being the fundamental tau-function expressed by a finite sum

$$f = \sum_{\mu=0,1} \exp\left[\sum_{i=1}^{N} \mu_i\left(\xi_i + \pi\mathrm{i}\right) + \sum_{1\le i<j\le N} \mu_i\mu_j\gamma_{ij}\right], \tag{2.5a}$$

$$\xi_i = k_i y + \frac{3}{2k_i}\tau + \xi_{i0}, \quad (i = 1,2,...,N), \tag{2.5b}$$

$$\mathrm{e}^{\gamma_{ij}} = \frac{(k_i - k_j)^2(k_i^2 - k_ik_j + k_j^2)}{(k_i + k_j)^2(k_i^2 + k_ik_j + k_j^2)}, \quad (i,j = 1,2,...,N; i \ne j). \tag{2.5c}$$

Here, k_i and ξ_{i0} are arbitrary complex parameters, and N is an arbitrary positive integer. The notation $\sum_{\mu=0,1}$ implies the summation over all possible combinations of $\mu_1 = 0,1,\mu_2 = 0,1,...,\mu_N = 0,1$. The bilinear operators D_τ and D_y in (2.4) are defined by

$$D_\tau^m D_y^n f\cdot g = \left(\frac{\partial}{\partial\tau} - \frac{\partial}{\partial\tau'}\right)^m \left(\frac{\partial}{\partial y} - \frac{\partial}{\partial y'}\right)^n f(y,\tau)g(y',\tau')\Big|_{\tau'=\tau,\, y'=y}, \quad (m,n = 0,1,2,...).$$

The above expression for u will be shown to represent the non-periodic N-cusp soliton solution for the real parameters k_j and ξ_{j0}. The former parameters are related to the amplitudes of solitons whereas the latter ones represent the phases of solitons. The cusped periodic wave solutions can be constructed by replacing these real parameters with the pure imaginary ones, i.e., $k_j \to \mathrm{i}k_j, \xi_{j0} \to \mathrm{i}\xi_{j0}$ $(j = 1,2,...,N)$. Theorem 2.1 is proved by a sequence of steps, which will be detailed in [9].

2.2. Soliton solutions

2.2.1. Cusp soliton

Here, we explore the properties of soliton solutions for both the non-periodic and periodic cases. In particular, we show that soliton solutions take the form of cusp solitons. The tau-functions for the one-soliton solution are given by (2.4) and (2.5) with $N = 1$ and $k_1, \xi_1 \in \mathbb{R}$. They read

$$f = 1 - \mathrm{e}^{\xi}, \quad g = 1 + 4\mathrm{e}^{\xi} + \mathrm{e}^{2\xi}, \quad \xi = ky + \frac{3}{2k}\tau + \xi_0, \tag{2.6}$$

where we have put $\xi = \xi_1, k = k_1$ and $\xi_0 = \xi_{10}$ for simplicity. The parametric representation of the solution follows from (2.3) and (2.6). It can be written in the form

$$u = -\frac{9}{2k^2}\frac{2\cosh\xi + 1}{(\cosh\xi + 2)^2}, \tag{2.7a}$$

$$X \equiv x + \frac{3}{2k^2}t + x_0 = \frac{\xi}{k} - \frac{3}{k}\frac{\sinh\xi}{\cosh\xi + 2}, \tag{2.7b}$$

where the traveling-wave coordinate X has been introduced for convenience in which x_0 is an arbitrary real constant. A typical profile of u is depicted on the left panel of figure 1 as a function of X. It represents a cusp soliton with the amplitude $3/(2k^2)$ and the velocity $3/(2k^2)$. To see the structure of the singularity in more detail, we compute the X derivative of u from (2.7) and obtain

$$u_X = \frac{9}{k}\frac{1}{\tanh\frac{\xi}{2}}\frac{1}{\cosh\xi + 2}. \tag{2.8}$$

Near the trough $X = 0$ ($\xi = 0$), one estimates that $u_X \sim 6/(k\xi), X \sim \xi^5/(180k)$, and hence $\lim_{X\to\pm 0} u_X = \lim_{X\to\pm 0}(218/5k^6)^{1/5}/X^{1/5} = \pm\infty$, showing the appearance of the cusp.

2.2.2. Cusped periodic wave

The cusped periodic wave solution is obtained formally from (2.7) if one replaces the parameters as $k \to \mathrm{i}k, \xi \to \mathrm{i}\xi$. It reads in the form

$$u = \frac{9}{2k^2}\frac{2\cos\xi + 1}{(\cos\xi + 2)^2}, \tag{2.9a}$$

$$X \equiv x - \frac{3}{2k^2}t + x_0 = \frac{\xi}{k} - \frac{3}{k}\frac{\sin\xi}{\cos\xi + 2}. \tag{2.9b}$$

The expression corresponding to (2.8) becomes

$$u_X = -\frac{9}{k}\frac{1}{\tan\frac{\xi}{2}}\frac{1}{\cos\xi + 2}. \tag{2.10}$$

It represents the cusped periodic wave with the period $2\pi/k$. The cusp singularity appears at the crest of the periodic wave. The middle panel of figure 1 shows the profile of a cusped periodic wave with the period $2\pi\sqrt{2/3}$.

It is important to observe that (2.9) belongs to a class of singular traveling waves. Actually, the traveling wave ansatz $u = u(X),\ X = x - ct - x_0$ ($c, x_0 \in \mathbb{R}$) reduces Eq.

(2.1) to an ODE $-cu_{XX} = 3u/2 - uu_{XX} - u_X^2/4$. Integrating this equation once with respect to X, we obtain

$$\left(\frac{du}{dX}\right)^2 = 2u - \frac{4d}{|u-c|^{1/2}} + 4c, \tag{2.11}$$

where $d \in \mathbb{R}$ is an integration constant. One can confirm that (2.9) indeed satisfies Eq. (2.11) with $d = -c^{3/2}$ and $c = 3/(2k^2)$.

2.2.3. Peaked periodic wave

Equation (2.11) exhibits smooth periodic solutions if $c > 0$ and $0 < d < c^{3/2}$. In particular, in the limit of $d \to c^{3/2}$, the periodic wave reduces to an infinitesimal wave of the form $u \sim a\cos\sqrt{3/2c}X,\ |a| << 1,\ a \in \mathbb{R}$. In the limit $d \to 0$, on the other hand, it reduces to the peaked periodic wave with parabolic profile

$$u = \frac{1}{2}(X^2 - 4c), \quad X \in [-\sqrt{6c}, \sqrt{6c}], \tag{2.12}$$

periodically continued beyond the interval $[-\sqrt{6c}, \sqrt{6c}]$. It should be remarked that the solution (2.12) can be derived directly by integrating Eq. (2.11) with $d = 0$. See the right panel of figure 1. The phase plane analysis of Eq. (2.11) exhibits a variety of periodic solutions. The detail will be reported elsewhere.

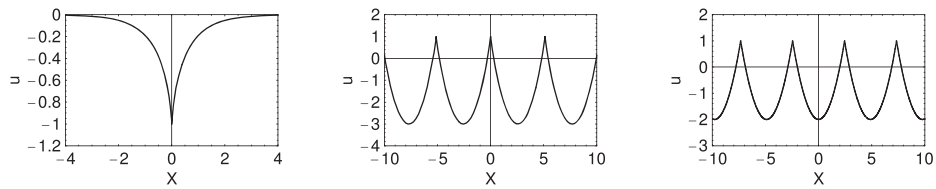

Figure 1 The profiles of the cusp soliton, cusped periodic wave and peaked periodic wave solutions with the parameter $k = \sqrt{3/2}$. Left: Cusp soliton. Middle: Cusped periodic wave, Right: Peaked periodic wave with $c = 1$.

3. Parametric solutions of equation (1.6)

In this section, we present the parametric multisoliton solutions of equation (1.6). First, we observe that equation (1.6) exhibits two exact solutions, $u = -x/4 + c_1 t + c_2$ and $u = x/2 + c_1 t + c_2$, where c_1 and c_2 are arbitrary constants. We shall show that soliton solutions of equation (1.6) asymptotically approach either these straight lines or $u = 0$ as $|x| \to \infty$. Hence, the zero boundary conditions $u \to 0, |x| \to \infty$ are not specified in advance.

3.1. Parametric solutions

Here, we establish the following theorem.

Theorem 3.1. *Equation (1.6) admits the parametric representation for the multisoliton solutions*

$$u = \frac{1}{2}\left(\ln\frac{f^2}{g}\right)_\tau, \tag{3.1a}$$

$$x = y - (\ln f^4 g)_\tau + y_0, \tag{3.1b}$$

where the tau-functions $g = g(y,\tau)$ and $f = f(y,\tau)$ are given respectively by (2.4) and (2.5) in which the variable τ is replaced by $2\tau/3$.

3.2. Soliton solutions

The tau-functions for the one-soliton solution is given by (2.4) and (2.5) with τ replaced by $2\tau/3$. They read

$$f = 1 - \mathrm{e}^{\xi}, \quad g = 1 + 4\mathrm{e}^{\xi} + \mathrm{e}^{2\xi}, \quad \xi = ky + \frac{\tau}{k} + \xi_0. \tag{3.2}$$

Substitution of these expressions into (3.1) yields the parametric representation of the one-soliton solution

$$u = \frac{3}{2k}\frac{\coth\frac{\xi}{2}}{\cosh\,\xi + 2}, \tag{3.3a}$$

$$X \equiv x + \frac{t}{k^2} + x_0 = \frac{\xi}{k} - \frac{3}{2k}\frac{\mathrm{e}^{\frac{\xi}{2}}(\mathrm{e}^{\xi}+3)}{\sinh\frac{\xi}{2}\,(\cosh\,\xi + 2)} + y_0. \tag{3.3b}$$

It follows from (3.3a, b) by a direct computation that

$$\frac{du}{dX} = -\frac{3(\cosh\,2\xi + 2\,\cosh\,\xi + 3)}{\cosh\,3\xi + 6\,\cosh\,2\xi + 39\,\cosh\,\xi + 26}. \tag{3.3c}$$

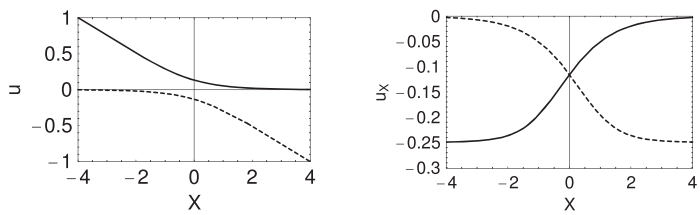

Figure 2. The profiles of an unbounded solution and its X derivative with the parameters $k = 1.0, y_0 = 3$. Left: u. Right: u_X.

The typical profiles of u and u_X are depicted in figure 2 as a function of X. The solution exhibits the different features depending on the range of the parameter ξ. Specifically, the solution represented by the solid curve in figure 2 corresponds to $0 < \xi < \infty$ whereas that of the dashed curve corresponds to $-\infty < \xi < 0$. The former (latter) solution diverges when X tends to $-\infty$ $(+\infty)$, and asymptotically approaches a straight line $u = -X/4$ since $u \sim 1/(k\xi), X \sim -4/(k\xi)$ near $\xi = 0$. We observe that $\xi = 0$ is the zero of the tau-function f from (3.2) which separates two branches of the solutions. One can show that $-1/4 < u_X < 0$ for any finite X. Recall that $u = -X/4$ is an exact solution of equation (1.6). It can be seen from figure 2 that for each curve, u_X takes the form of a kink. Note also that if $u(x,t)$ is a solution of equation (1.6), then $-u(-x,-t)$ satisfies equation (1.6) as well. This symmetry relation is manifested clearly in figure 2 in which the solution represented by the solid curve is mapped to that represented by the dashed curve by means of the transformation $u(X) \to -u(-X)$.

Another divergent solution is produced if one shifts the parameter ξ_0 as $\xi_0 \to \xi_0 + \mathrm{i}\pi$. Then, the tau-functions f and g from (3.2) become

$$f = 1 + \mathrm{e}^{\xi}, \quad g = 1 - 4\mathrm{e}^{\xi} + \mathrm{e}^{2\xi}, \quad \xi = ky + \frac{\tau}{k} + \xi_0. \tag{3.4}$$

The parametric representation of the solution corresponding to (3.3) is given by

$$u = \frac{3}{2k}\frac{\tanh\frac{\xi}{2}}{2 - \cosh\,\xi}, \tag{3.5a}$$

$$X \equiv x + \frac{t}{k^2} + x_0 = \frac{\xi}{k} - \frac{3}{2k}\frac{\mathrm{e}^{\frac{\xi}{2}}(3 - \mathrm{e}^{\xi})}{\cosh\,\frac{\xi}{2}\,(2 - \cosh\,\xi)} + y_0, \tag{3.5b}$$

$$\frac{du}{dX} = \frac{3(\cosh\,2\xi - 2\,\cosh\,\xi + 3)}{\cosh\,3\xi - 6\,\cosh\,2\xi + 39\,\cosh\,\xi - 26}. \tag{3.5c}$$

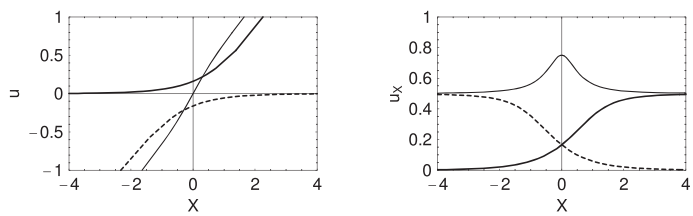

Figure 3. The profiles of an unbounded solution and its X derivative with the parameters $k = 1.0, y_0 = 3$. Left: u. Right: u_X.

The profiles of u and u_X for the same values of the parameters as those of figure 2 are shown in figure 3. The solution has three branches according to the range of ξ. The solid, thin solid and dashed curves represent the solutions for $-\infty < \xi < -s, -s < \xi < s$ and $s < \xi < \infty$, respectively, where s is a positive solution of the transcendental equation $\cosh \xi = 2$, i.e., $s \simeq 1.317$. This coincides with the positive zero of the tau-function g from (3.4), i.e., $\xi = \ln(2 + \sqrt{3})$. When compared with figure 2, a new branch of the solution appears which is represented by the thin solid curve. The corresponding expression of u_X takes the form of a bright soliton on a constant background. Note that the inequality $1/2 < u_X < 3/4$ holds for finite X. See the right panel of figure 3.

4. Parametric solutions of equation (1.7)

We modify equation (1.7) by means of the linear transformation $(u, x, t) \to (U, X, T)$ according to $U = \frac{\beta}{\alpha} u + 1, X = \frac{\sqrt{-\beta}}{\alpha} x + \frac{\alpha}{\sqrt{-\beta}} t, T = \frac{\alpha}{\sqrt{-\beta}} t$. Then, we find that it is expressed in terms of the new variables as $U_{XT} = U - 1 - U^2 U_{XX} - U U_X^2$. Subsequently, we replace the variables U, X, T by $u, \mathrm{i}x, -\mathrm{i}t$, respectively, and obtain the basic equation that we consider here:

$$u_{xt} = u - 1 + u^2 u_{xx} + u u_x^2. \tag{4.1}$$

In this section, we solve equation (4.1) under the boundary condition $u \to 1, |x| \to \infty$ which corresponds to non-periodic solutions.

4.1. Parametric solutions

Here, we establish the following theorem.

Theorem 4.1. *Equation (4.1) admits the parametric representation for the multisoliton solutions*

$$u = 1 + \mathrm{i} \left(\ln \frac{\bar{f}}{g} \right)_\tau, \tag{4.2a}$$

$$x = y - \tau - \mathrm{i} \ln \frac{\bar{f}}{g} - (\ln \bar{f} g)_\tau + y_0, \tag{4.2b}$$

where $\bar{f}$ and g are tau-functions given by

$$\bar{f} = \sum_{\mu=0,1} \exp \left[\sum_{i=1}^{N} \mu_i \left(\xi_i + d_i - \frac{\pi}{2} \mathrm{i} \right) + \sum_{1 \le i < j \le N} \mu_i \mu_j \gamma_{ij} \right], \tag{4.3a}$$

$$g = \sum_{\mu=0,1} \exp \left[\sum_{i=1}^{N} \mu_i \left(\xi_i - d_i + \frac{\pi}{2} \mathrm{i} \right) + \sum_{1 \le i < j \le N} \mu_i \mu_j \gamma_{ij} \right], \tag{4.3b}$$

with

$$\xi_i = p_i y + \frac{1}{p_i}\,\tau + \xi_{i0}, \quad (i = 1, 2, ..., N), \tag{4.3c}$$

$$\mathrm{e}^{d_i} = \sqrt{\frac{1 + \mathrm{i}p_i}{1 - \mathrm{i}p_i}}, \quad (i = 1, 2, ..., N), \tag{4.3d}$$

$$\mathrm{e}^{\gamma_{ij}} = \left(\frac{p_i - p_j}{p_i + p_j}\right)^2, \quad (i, j = 1, 2, ..., N; i \neq j). \tag{4.3e}$$

Here, p_i and ξ_{i0} are arbitrary complex parameters.

If one puts $p_i = \tan\,\theta_i$, then the expression of d_i from (4.3*d*) simplifies to $d_i = \mathrm{i}\theta_i$. This parametrization is found to be very useful in constructing cusp and breather solutions.

The solutions given by (4.2) become complex-valued functions for complex parameters p_i and ξ_{i0}. If one imposes the conditions $\bar{f} = g^*, \bar{g} = f^*$ for the tau-functions with the asterisk being the complex conjugate, then, (4.2) gives rise to real solutions characterized by a single tau-function g. It reads

$$u = 1 + \mathrm{i}\left(\ln\frac{g^*}{g}\right)_\tau, \tag{4.4a}$$

$$x = y - \tau - \mathrm{i}\ln\frac{g^*}{g} - (\ln g^* g)_\tau + y_0. \tag{4.4b}$$

The conditions mentioned above for the tau-functions are realized if one takes the real values for the parameters p_i and ξ_{i0} which would lead to cusp soliton solutions, as will be exemplified below. Another choice is possible by putting $N = 2M$ and $p_{2i-1} = p_{2i}^*, \xi_{2i-1} = \xi_{2i}^*$ $(i = 1, 2, ..., M)$, where M is a positive integer. The resulting solutions would be shown to take the form of breather solutions.

4.2. Soliton solutions

4.2.1. Cusp soliton

The tau-function g for the one-soliton solution is given by (4.3*b*) with $N = 1$. It can be written in the form

$$g = 1 + \mathrm{i}\,\mathrm{e}^{\xi - d}, \quad \mathrm{e}^d = \sqrt{\frac{1 + \mathrm{i}p}{1 - \mathrm{i}p}}, \quad \xi = py + \frac{1}{p}\,\tau + \xi_0, \tag{4.5}$$

where p and ξ_0 are real parameters. If we put $p = \tan\,\theta$ $(0 < \theta < \pi/2)$, then $d = \mathrm{i}\theta$ and $g = 1 + \mathrm{i}\mathrm{e}^{\xi - \mathrm{i}\theta}$. Introducing g into (4.35) yields a one-soliton solution

$$u = 1 + \frac{\cos\,\theta}{\tan\,\theta}\frac{1}{\cosh\,\xi + \sin\,\theta}, \tag{4.6a}$$

$$X \equiv x + \frac{1}{\sin^2\theta}\,t + x_0 = \frac{\xi}{\tan\theta} - \frac{1}{\tan\theta}\frac{\sinh\xi}{\cosh\xi + \sin\theta} - 2\,\tan^{-1}\left(\frac{\cos\theta}{1+\sin\theta}\,\tanh\frac{\xi}{2}\right). \tag{4.6b}$$

Here, the constant y_0 has been chosen such that $\xi = 0$ corresponds to $X = 0$. Although the expression (4.6) represents a bounded solution, it has a cusp at the crest. To see this, we compute the X derivative of u to obtain

$$u_X = \frac{u_\xi}{X_\xi} = -\frac{\cos\theta}{\sinh\xi}. \tag{4.6c}$$

On the other hand, the coordinate X from (4.6b) has an expansion $X = \kappa\,\xi^3 + O(\xi^5)$ near $\xi = 0$, where $\kappa = \frac{\cos\theta + \cot\theta}{3(1+\sin\theta)^3}$. Thus, $u_X \sim -\kappa^{1/3}\,\cos\theta\,X^{-1/3}$, implying that $\lim_{X\to\pm 0} u_X = \mp\infty$.

The profile of the cusp soliton is plotted as a function of X on the left panel of figure 4. It represents a singular pulse propagating to the left at a constant velocity $1/\sin^2\theta$ on the coordinate system at rest.

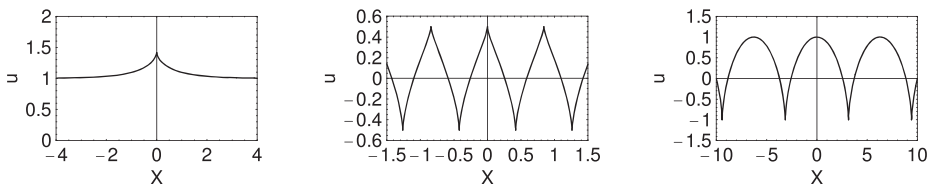

Figure 4. The profiles of the cusp soliton and cusped periodic wave solutions. Left: Cusp soliton with the parameter $\theta = \pi/4$. Middle: Cusped periodic wave with the parameter $\theta = \cosh^{-1} 2$. Right: Cycloid.

4.2.2. Cusped periodic wave

The cusped periodic wave solution is obtained formally from the cusp soliton solution (4.6) if one replaces the parameters ξ and θ by $\mathrm{i}\xi$ and $\pi/2 + \mathrm{i}\theta$, respectively. The parametric solution (4.6) then becomes

$$u = 1 - \frac{\sinh\theta}{\coth\theta}\frac{1}{\cos\xi + \cosh\theta}, \tag{4.7a}$$

$$X \equiv x + \frac{1}{\cosh^2\theta}\,t + x_0 = \frac{\xi}{\coth\theta} - \frac{1}{\coth\theta}\frac{\sin\xi}{\cos\xi + \cosh\theta} - 2\,\tan^{-1}\left(\frac{\sinh\theta}{1+\cosh\theta}\,\tan\frac{\xi}{2}\right), \tag{4.7b}$$

for $\xi \in (-\pi, \pi)$. The solution (4.7) can be periodically continued beyond the interval $(-\lambda/2, \lambda/2)$ with $\lambda = 2\pi(1 - \tanh\theta)$. It turns out that (4.7) represents a cusped periodic

wave with the amplitude $1/\cosh\theta$ and the period λ. Its typical profile is depicted on the middle panel of figure 4. Since $u_X = \sinh\theta/\sin\xi$, the cusp appears both at the crest and at the trough in marked contrast to the periodic traveling wave solution of equation (1.5) shown on the middle panel of figure 1 in which the cusp appears only at the crest of the wave.

Last, we demonstrate that an intriguing result is obtained from a special limit of (4.7). To be more specific, let $\xi = \pi + \theta\cot(\phi/2)$ $(\phi \in \mathbb{R})$, and take the limit $\theta \to 0$. Then, (4.7) reduces to

$$u = \cos\phi, \quad X \equiv x + t + x_0 = \phi + \sin\phi. \tag{4.8}$$

The profile of (4.8) is plotted on the right panel of figure 4. It follows from (4.8) that $u_X = -\tan(\phi/2)$, which determines the position of the cusp, i.e., $X = \pi \pmod{2\pi}$. The parametric solution (4.8) represents the cycloid which is familiar to us in geometry. It satisfies an ODE, $(du/dX)^2 = (1-u)/(1+u)$. Actually, if we seek the traveling wave solution of the form $u = u(X), X = x - ct + x_0$ $(c, x_0 \in \mathbb{R})$, then we see that Eq. (4.1) can be recast to a nonlinear ODE, $(du/dX)^2 = -(u^2 - 2u + d)/(u^2 + c)$ $(d \in \mathbb{R})$. In the case of $c = -1$ and $d = 1$, this equation simplifies to an ODE mentioned above. Recall that the conventional representation of the cycloid is given by $x = a(t - \sin t), y = a(1 - \cos t)$, $(a > 0, t \in \mathbb{R})$ in the (x, y) plane, and the transformation of (4.8) to this form can be made simply by shifting the variables u, X and ϕ by $u - 1$, $X + \pi$ and $\phi + \pi$, respectively. It is interesting to observe that the expression $-u$ from (4.8) coincides with the surface profile of Gerstner's trochoidal wave which has been derived more than 200 years ago in the theory of deep gravity waves [10, 11]. Last, we point out that smooth periodic wave solutions exist if $c > 0$ and $d < 1$ in the above ODE.

4.2.3. Breather

The breather solutions are obtained following the recipe described in the last sentence in section 4.1. To show this, we find it convenient to introduce the new parameters according to the relations

$$\xi_j = \eta_j + \mathrm{i}\chi_j, \quad \xi_{j0} = \lambda_j + \mathrm{i}\mu_j, \quad p_j = \tan\theta_j = a_j + \mathrm{i}b_j, \quad \theta_j = \alpha_j + \mathrm{i}\beta_j, \quad (j = 1, 2, ..., N). \tag{4.9}$$

The parameters a_j and b_j are expressed in terms of α_j and β_j as

$$a_j = \frac{\frac{1}{2}\sin 2\alpha_j}{\cosh^2\beta_j - \sin^2\alpha_j}, \quad b_j = \frac{\frac{1}{2}\sinh 2\beta_j}{\cosh^2\beta_j - \sin^2\alpha_j}, \quad (j = 1, 2, ..., N). \tag{4.10}$$

It turns out from (4.10) that $a_j/b_j = \sin 2\alpha_j/\sinh 2\beta_j$. This quantity characterizes the feature of the solution.

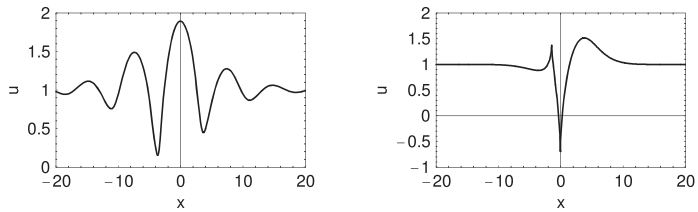

Figure 5. The profiles of the breather solutions. Left: The smooth breather with the parameters $p_1 = p_2^* = \tan(\pi/6 + \mathrm{i}), \xi_{10} = \xi_{20}^* = 0$. Right: The singular breather with the parameters $p_1 = p_2^* = \tan(\pi/6 + 0.2\,\mathrm{i}), \xi_{10} = \xi_{20}^* = 0$.

Here, we consider the single breather solution. The corresponding tau-function is given by (4.3b) with $N = 2$. We put $\xi_1 = \xi_2^* = \eta + \mathrm{i}\chi, p_1 = p_2^* = \tan\theta = a + \mathrm{i}b, \theta = \alpha + \mathrm{i}\beta, \xi_{10} = \xi_{20}^* = \lambda + \mathrm{i}\mu, \delta = (b/a)^2$. Then, the tau-function g can be expressed in the form

$$g = 1 + \mathrm{i}\,\mathrm{e}^{\eta+\beta+\mathrm{i}(\chi-\alpha)} + \mathrm{i}\,\mathrm{e}^{\eta-\beta-\mathrm{i}(\chi+\alpha)} + \delta\,\mathrm{e}^{2\eta-2\mathrm{i}\alpha}, \tag{4.11a}$$

with

$$\eta = ay + \frac{a}{a^2+b^2}\,\tau + \lambda, \quad \chi = by - \frac{b}{a^2+b^2}\,\tau + \mu. \tag{4.11b}$$

The parametric representation of the solution is given by (4.4) with the tau-function g from (4.11a). The explicit form of the solution is, however too complicated to write down here. The profile of the smooth breather solution at $t = 0$ is depicted on the left panel of figure 5 as a function of x for the specified values of the parameters. It represents an oscillating pulse on a constant background. The smoothness of the solution depends on the parameter $1/\sqrt{\delta} = a/b$ ($a > 0, b > 0$). A detailed analysis reveals that the smooth solutions are produced if the condition $a/b < \cos\alpha/\cosh\beta$ ($0 < \alpha < \pi/2, \beta > 0$) is satisfied. In the present example, $a/b = 0.239, \cos\alpha/\cosh\beta = 0.561$ ($\alpha = \pi/6, \beta = 1.0$). As for the analogous conditions for the smooth breather solutions of the SP and modified SP equations, one can refer to Refs. [7, 12].

If the value of the parameter a/b exceeds certain critical value, then the singularities of the solutions appear in the form of cusps. The amplitude of the solution is, however finite since $g \neq 0$ (or $g^* g > 0$) for arbitrary values of η and χ, as can be confirmed by using (4.11b). The formation of cusps is exemplified on the right panel of figure 5 for the specified values of the parameters. In this example, $a/b = 2.11$ and $\cos\alpha/\cosh\beta = 0.849$, so that the condition for the smoothness is violated.

References

[1] Hone A N W, Novikov V and Wang J P 2018 Generalizations of the short pulse equation *Lett. Math. Phys.* **108** 927-947

[2] Schäfer T and Wayne C E 2004 Propagation of ultra-short optical pulses in cubic nonlinear media *Physica D* **196** 90-105

[3] Matsuno Y 2009 Soliton and periodic solutions of the short pulse model equation *Handbook of Solitons: Research, Technology and Applications* ed S P Lang and H Bedore (New York: Nova) pp. 541-585

[4] Vakhnenko V A 1992 Solitons in a nonlinear model media *J. Phys. A: Math. Gen.* **25** 4181-4187

[5] Hunter J K and Saxton R 1991 Dynamics of director fields *SIAM J. Appl. Math.* **51** 1498-1521

[6] Sakovich S 2016 Transformation and integrability of a generalized short pulse equation *Commun. Nonlinear Sci. Numer. Simul.* **39** 21-28

[7] Matsuno Y 2016 Integrable multi-component generalization of a modified short pulse equation *J. Math. Phys.* **57** 111507

[8] Manna M A and Neveu A 2001 Short-wave dynamics in the Euler equations *Inverse Problems* **17** 855-861

[9] Matsuno Y 2020 Parametric solutions of the generalized short pulse equations *J. Phys. A: Math. Theor.* **53** 105202

[10] Gerstner F 1809 Theorie der Wallen *Annl. Phys.* **32** 412-445

[11] Henry D 2008 On Gerstner's water wave *J. Nonl. Math. Phys.* **15** Suppl 2 87-95

[12] Sakovich A and Sakovich S 2006 Solitary wave solutions of the short pulse equation *J. Phys. A: Math. Gen.* **39** L361-L367